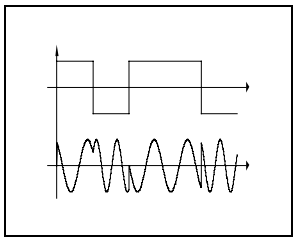

3

Frequency Shift Keying

The previous chapter contained a brief introduction to the DSC-ASIC application. The purpose of this chapter is then to extend this description with a study of the most fundamental aspects of Frequency Shift Keying modulation. The chapter is also meant as a brief survey for readers unfamiliar with this subject and should preferably enable these readers to understand the decisions made, concerning choice of algorithms and architecture. The main purpose of this chapter is to introduce Noncoherent Binary Frequency Shift Keying. To introduce this in a natural way, the starting point of this discussion is taken in Coherent Frequency Shift Keying as the theory of this modulation technique is easier to understand. The reason for this starting point is that the theoretical procedure is similar when describing both coherent FSK and the non-coherent counterpart.

3.1 Overview

Digital Modulation and Demodulation is basically the process by which digital symbols are transformed into waveforms $s_i(t)$ that are compatible with the characteristics of a transmission channel. In the case of Frequency Shift Keying the digital symbols are converted into distinct frequencies for a constant duration. This duration is called the baud-rate and is defined as the number of digital symbols per second. Frequency Shift Keying can be divided into different classes according to the number of digital symbols, the relation between the corresponding frequencies and the phase of these frequencies. This is illustrated in Fig. 3.1

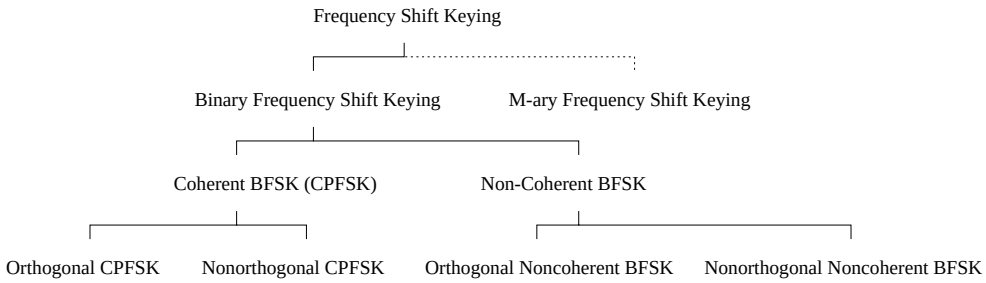

Fig. 3.1 *Overview over different classifications of FSK modem techniques that will be described here. The classes lowermost are the ones considered theoretically and practically in the following. (CPFSK: Continuous Phase FSK)*

As can be seen in Fig. 3.1 Frequency Shift Keying can in general be divided into Binary FSK and M-ary FSK, where the number of different Digital symbols equals two in the Binary case. M-ary FSK Signaling (Number of digital symbols > 2) is a broad subject which will be avoided in this context, as the purpose of this appendix is to describe binary FSK techniques.

Binary Frequency Shift Keying can then be divided into Coherent FSK and Non-coherent FSK as illustrated in Fig. 3.1. The difference between these two signalling forms is that in the coherent case the phase of the tones $s_i(t)$ describing each symbol is selected based on the phase of the tone describing the previous symbol. Thereby the phase of the transmitted signal can remain continuous which also gives the name to this signalling form: Continuous Phase FSK (CPFSK). Phase Continuity is not necessarily maintained in the non-coherent case, where the phase of the tones describing two successive digital symbols are independent of each other. The choice of coherence versus noncoherent transmission may very well depend on the circuit generating the FSK signal. This is illustrated in Fig. 3.2. (Note that coherent versus noncoherent *reception* may also depend on the characteristics of the transmission channel, this shall be seen later on)

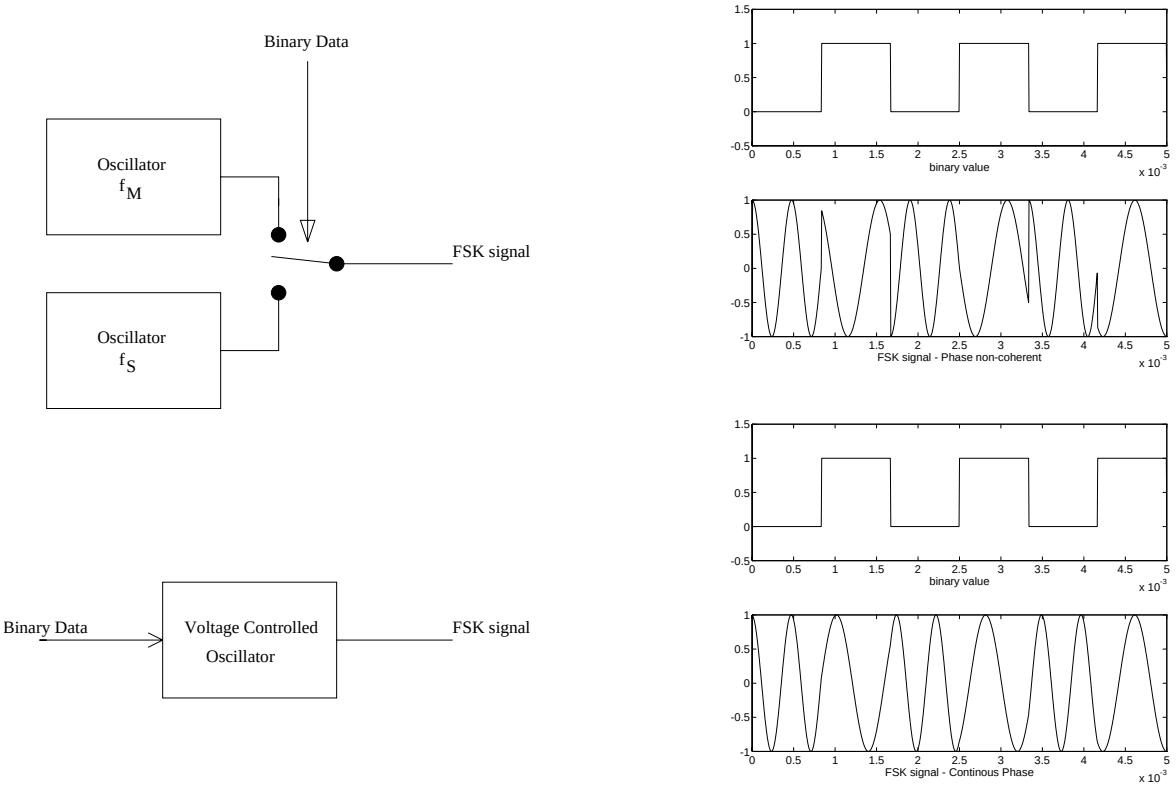

Fig. 3.2 *FSK signal generation models. Uppermost: Non-Coherent Binary FSK signal generation circuit consisting of two independent oscillations and a switching circuit controlled by the digital waveform. Lowermost: Coherent Binary FSK signal generator consisting of a Voltage Controlled Oscillator controlled by the Binary data where digital 1 then corresponds to e.g 5V and digital 0 corresponds to 0V.*

The difference between Coherent and Noncoherent FSK signal generation is shown in Fig. 3.2. The upper circuit generates a non-coherent FSK signal. The signal is seen at the right, where the phase of the tones describing each digital symbol does *not* depend on the phase of the previous symbol. In a receiver it is therefore not possible to know the exact phase of the sinusoid describing a new symbol, and discrimination between the two corresponding tone frequencies have to disregard phase information thereby reducing performance. In the lower circuit the frequency of the transmitted signal is changed in a phase continuous matter, thereby avoiding phase-jumps. In this signal form

the phase of a new symbol will always depend on the phase of the previous symbol. Discrimination between the two tone frequencies can thereby include phase information since an exact prototype of the two waveforms describing the digital symbols can be constructed in the receiver, based on the phase of the previous symbol.

This is not the only difference between the two signalling forms! In Fig. 3.5 the frequency content of the transmitted signal is plotted for a 100 bit pseudo-random pattern at a signalling rate of 1200 baud. The two tone frequencies equals f_M=1300 and f_S=2100 as prescribed in the CCITT V.23 standard.

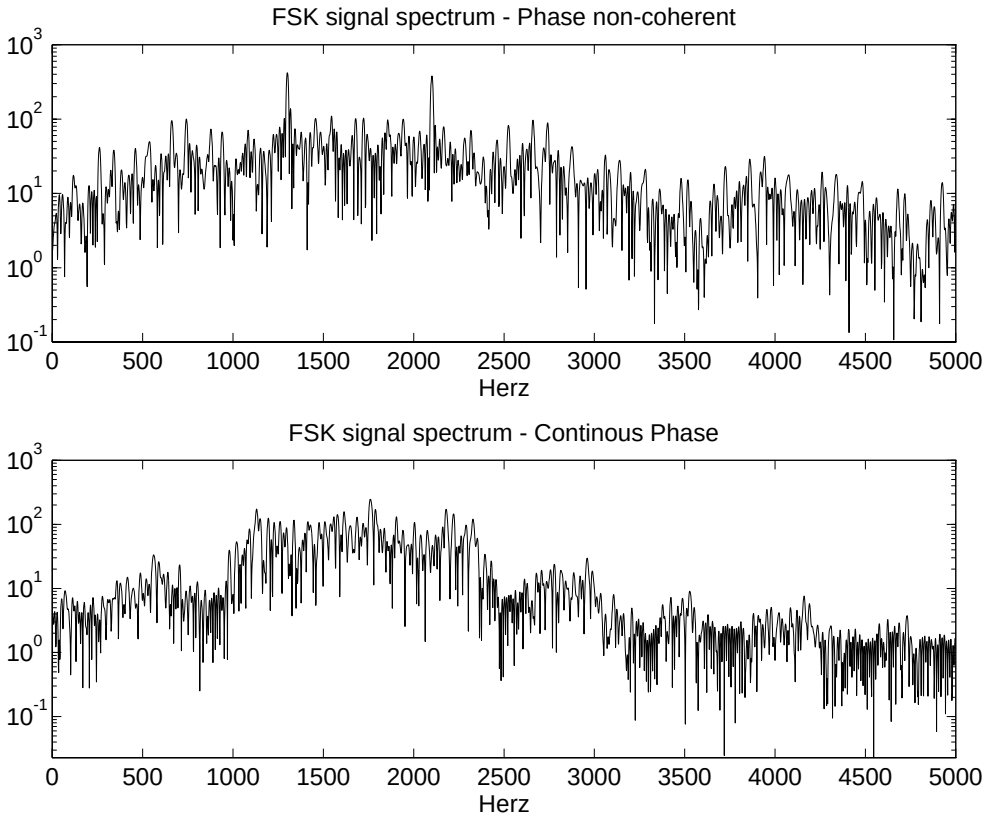

Fig. 3.5 *Frequency content of 100 bit pseudo random FSK signals. Uppermost Phase discontinuous FSK. Lowermost: Phase continuous FSK.*

As can be seen in Fig. 3.5 the CPFSK signals process a smaller frequency bandwidth than phase discontinuous FSK. This is also intuitively correct as the "phase-jumps" in non-coherent FSK must bring about higher frequency content than if the phase changes smoothly as in coherent FSK. This fact also becomes evident when considering the phase coherent vs. noncoherent signal waveforms when these have been passed trough e.g. a speech transmission channel with a typical frequency bandwidth: 300-3400Hz. Such a system is modelled in the following figure where coherent and non-coherent waveforms for alternating 0/1 bit-patterns is filtered trough a linear phase filter. I.e the group delay is maintained constant and the phase of the signal remains undistorted.

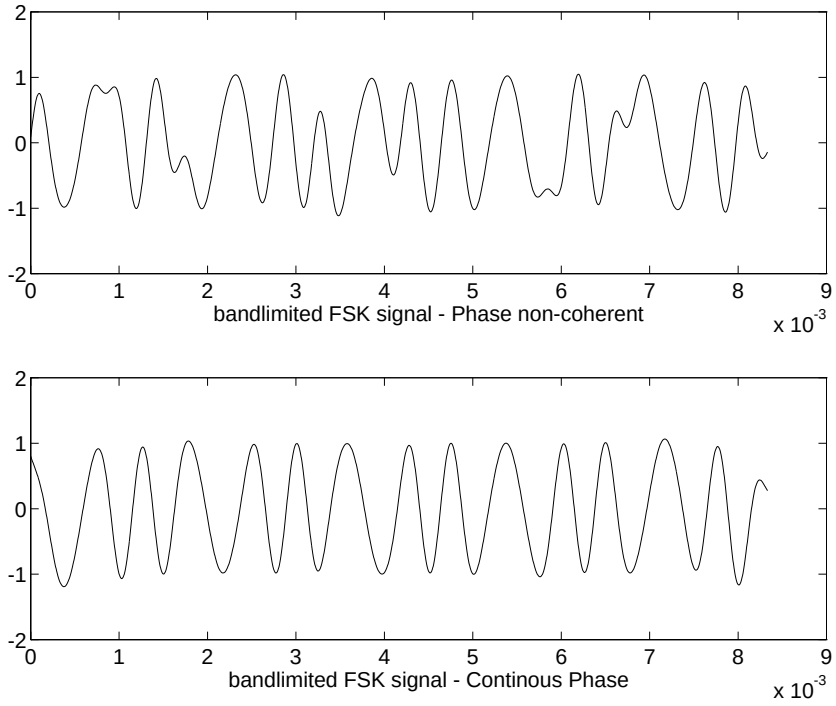

Fig. 3.6 *FSK signals, band-limited to the frequency range 300-3400Hz using a linear phase filter.*

As can be seen in Fig. 3.6 the Phase-continuous FSK Signal remains almost undistorted when passed though a band-pass channel opposed to the phase-noncoherent FSK signal which is transmitted more distorted. The effect is as expected, the "sharp" signal edges is filtered out by the band limiting effect of the transmission channel, thereby making the signal look more distorted. This is the reason why phase continuity most often is remained in the transmitting media, as this kind of signals transmits most undistorted. The price to be paid for this is a more complex signal generation circuit as the change in frequency has to be performed with continuous phase thereby preserving "memory" in which the previous state has to be stored. For non-coherent signal generation this is unnecessary as seen in Fig. 3.2.

The previous discussion has served as a description of the properties of FSK signal generation. However a more varied picture is first obtained when taking the demodulation process into consideration also. In the following (Chapter C.2 and C.3) the theoretical obtainable error rates for orthogonal Binary FSK are derived. The corresponding derivations for non-orthogonal FSK signaling becomes rather unmanageable. Therefore these error rates are instead obtained my means of simulation (Chapter C.4).

3.2 Orthogonal Coherent FSK Demodulation

As described in Fig. 3.1 Coherent and Noncoherent Binary FSK can be divided further into orthogonal and non-orthogonal cases. The effect of this is most evident when considering the performance of the different modulation schemes in the presence of noise. Orthogonal signalling is obtained if the inner product of the two signal waveforms $s_1(t)$ and $s_2(t)$, representing digital 0 and 1 respectively, equals zero over one bit-period. I.e. if the integral of the product of the two waveforms $s_1(t)$ and $s_2(t)$ equals zero:

$$\textit{Orthogonality:} \quad \int_0^{T_b} s_1(t) \cdot s_2(t)\, dt = 0 \tag{3.1}$$

For coherent orthogonal signalling the transmitted waveforms are described as:

$$s_i(t) = \begin{cases} \sqrt{\frac{2E_b}{T_b}} \cos(2\pi f_i t), & 0 \le t \le T_b \\ 0, & \textit{elsewhere} \end{cases} \tag{3.2}$$

where i=1,2 and E_b is the transmitted signal energy per bit. Orthogonality is ensured by assuming that:

$$f_i = (n_c + i) \cdot \frac{1}{T_b}, \qquad \textit{for some fixed integer } n_c \textit{ and } i = 1, 2 \tag{3.3}$$

where frequency f_1 represents symbol 1, and transmission of frequency f_2 represents symbol 0. I.e the frequencies are integral multiples of the baud rate, meaning that an integral number of periods describe each symbol. The ideal demodulation scheme then consists of correlating the received signal with two prototype waveforms and decide in favor of the one which correlates "best", as shown in Fig. 3.7.

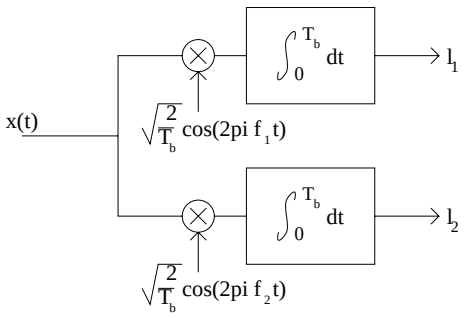

Fig. 3.7 *The Ideal Orthogonal Coherent FSK demodulation scheme.*

Suppose symbol 1 or frequency f_1 is transmitted, then a correct decision will be made by the receiver if $l_1 > l_2$. If however the noise is such that $l_2 > l_1$, the receiver erroneously decides in favor of symbol 0.

3.2.1 Error Rate

To calculate the probability of error it is necessary to calculate the probability density functions of the random variables L_1 and L_2 whose sample values are denoted by l_1 and l_2 respectively. When frequency f_1 is transmitted in the case of coherent orthogonal FSK the received signal x(t) is of the form:

$$x(t) = \sqrt{\frac{2E_b}{T_b}} \cos(2\pi f_1 t) + w(t), \qquad 0 \le t \le T_b \tag{3.4}$$

and the output of the correlator l_1 and l_2 then equal:

$$l_1 = \int_0^{T_b} \sqrt{\frac{2}{T_b}}\, x(t)\cos(2\pi f_1 t)\ , \qquad l_2 = \int_0^{T_b} \sqrt{\frac{2}{T_b}}\, x(t)\cos(2\pi f_2 t) \tag{3.5}$$

Considering the case where f_1 was transmitted and remembering the orthogonality condition this evaluates to:

$$l_1 = \sqrt{E_b} + w_1\ , \qquad l_2 = w_2 \tag{3.6}$$

where

$$w_i = \int_0^{T_b} w(t)\sqrt{\frac{2}{T_b}}\cos(2\pi f_i t)\ , \quad i = 1,\ 2 \tag{3.7}$$

This means that w_i, i=1,2 are samples of independent Gaussian random variables of zero mean and variance $N_0/2$ /Sklar 88/. The conditional probability density functions then equals:

$$f_{L_1|1}(l_1\,|\,1) = \frac{1}{\sqrt{2\pi N_0}}\exp\left[-\frac{(l_1 - \sqrt{E_b})^2}{2N_0}\right], \qquad f_{L_2|1}(l_2\,|\,1) = \frac{1}{\sqrt{2\pi N_0}}\exp\left[-\frac{l_2^2}{2N_0}\right] \tag{3.8}$$

The receiver makes an error if the sample value of l_2 exceeds the sample value of l_1 when symbol 1 was transmitted. The probability of this error can be obtained by integrating $f_{L2|1}(L_2|1)$ with respect to l_2 from l_1 to infinity and then averaging over all possible values of l_1, i.e:

$$P_{e1} = P(l_2 > l_1\,|\,1) = \int_0^{\infty} f_{L_1|1}(l_1\,|\,1)\left[\int_{l_1}^{\infty} f_{L_2|1}(l_2\,|\,1)\,dl_2\right]dl_1 \tag{3.9}$$

Substituting (3.8) into (3.9) can then be evaluated to equal /Haykin 83/:

$$P_{e1} = \frac{1}{\sqrt{\pi}}\int_{\sqrt{\frac{E_b}{2N_0}}}^{\infty} \exp(-z^2)\,dz \tag{3.10}$$

Which is recognized as the complementary error function /Sklar 88/:

$$P_{e1} = \frac{1}{2}\,erfc\left(\sqrt{\frac{E_b}{2N_0}}\right) \tag{3.11}$$

By symmetry it can be shown that P_{e0} has an equal probability thus the average probability of error equals:

$$P_e = \frac{1}{2}\,erfc\left(\sqrt{\frac{E_b}{2N_0}}\right) \tag{3.12}$$

This error probability can be plotted versus the E_b/N_0 ratio (see Fig. 3.10) but for the sake of comparison the case of noncoherent FSK is considered first.

3.3 Orthogonal Noncoherent FSK Demodulation

The binary Noncoherent FSK signal is as for coherent FSK defined by:

$$s_i(t) = \begin{cases} \sqrt{\frac{2E_b}{T_b}}\cos(2\pi f_i t) , & 0 \le t \le T_b \\ 0 , & elsewhere \end{cases} \quad (3.13)$$

where the frequency f_i equals one of two possible values f_1 and f_2. The transmission of frequency f_1 represents symbol 1, and the transmission of frequency of frequency f_2 represents symbol 0. Orthogonality is ensured as for coherent FSK and a look into the functionality of the ideal Noncoherent FSK demodulator reveals this as consisting of two paths that each evaluates the correlation between the received signal and two prototype sine waves at the specific tone frequencies /Sklar 88/, /Haykin 83/.

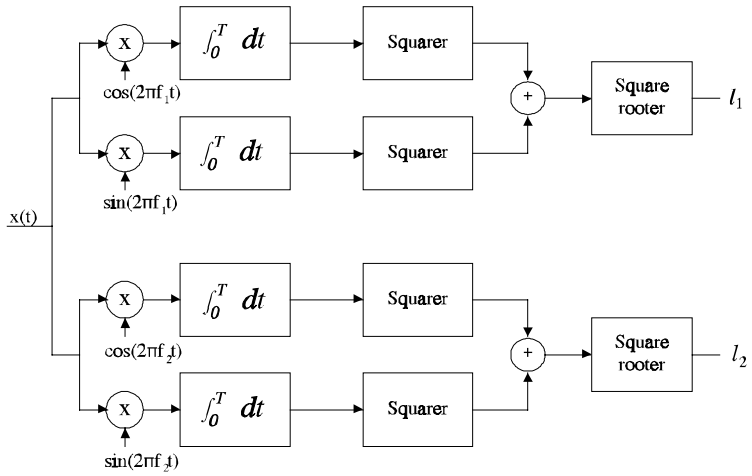

Fig. 3.8 *The noncoherent demodulation principle using correlators.*

l_1 and l_2 denotes the envelope samples of the upper and lower channels shown in Fig. 3.8. Then, if $l_1 > l_2$ the receiver decides in favor of symbol 1, and if $l_2 > l_1$ the receiver decides in favor of symbol 0. To describe the problem of noncoherent demodulation, the optimal error rate for this demodulation principle is derived under the assumption that the tone frequencies f_1 and f_2 are integral multiples of the bit rate $^1/_T$. Like the assumption in (3.3).

3.3.1 Error Rate

Suppose symbol 1 or frequency f_1 is transmitted. Then a correct decision will be made by the receiver if $l_1 > l_2$. If however the noise i such that $l_2 < l_1$, the receiver erroneously decides in favor of symbol 0. To calculate the probability of error, it is necessary to calculate the probability density functions of the random variables L_1 and L_2 whose sample values are denoted by l_1 and l_2 respectively.

When frequency f_1 is transmitted in the case of noncoherent FSK there is no synchronism between the receiver and transmitter and the received signal x(t) is of the form:

$$x(t) = \sqrt{\frac{2E_b}{T_b}}\cos(2\pi f_1 t + \theta) + w(t) , \qquad 0 \le t \le T_b \tag{3.14}$$

By using a well known trigonometric relation this becomes:

$$x(t) = \sqrt{\frac{2E_b}{T_b}}\cos\theta\cos(2\pi f_1 t) - \sqrt{\frac{2E_b}{T_b}}\sin\theta\sin(2\pi f_1 t) + w(t) , \qquad 0 \le t \le T_b \tag{3.15}$$

The signals $x_{s,i}$ and $x_{c,i}$ for i=1,2 then becomes:

$$x_{c,i} = \int_0^{T_b} \sqrt{\frac{2}{T_b}}\, x(t)\cos(2\pi f_i t)\, dt , \qquad x_{s,i} = \int_0^{T_b} \sqrt{\frac{2}{T_b}}\, x(t)\sin(2\pi f_i t)\, dt , \qquad i=1,2 \tag{3.16}$$

Now considering the case where f_1 was transmitted - remembering the orthogonality between f_1 and f_2 this evaluates to:

$$x_{c,1} = \sqrt{E_b}\cos\theta + w_{c,1} , \qquad x_{s,1} = \sqrt{E_b}\sin\theta + w_{s,1} \tag{3.17}$$

And the decision value l_1 then equals:

$$l_1 = \sqrt{x_{c,1}^2 + x_{s,1}^2} \tag{3.18}$$

In the other channel $x_{s,i}$ and $x_{c,i}$ evaluates to:

$$x_{c,2} = w_{c,2} , \qquad x_{s,2} = w_{s,2} \tag{3.19}$$

where $w_{c,i}$ and $w_{s,i}$ for i=1,2 in (3.17) and (3.19) are related to the noise w(t) as follows.

$$w_{c,i} = \int_0^{T_b} w(t) \sqrt{\frac{2}{T_b}}\cos(2\pi f_i t)\, dt , \qquad i=1,2 \tag{3.20}$$

and

$$w_{s,i} = \int_0^{T_b} w(t) \sqrt{\frac{2}{T_b}}\sin(2\pi f_i t)\, dt , \qquad i=1,2 \tag{3.21}$$

This means that $w_{c,i}$ and $w_{s,i}$, i=1,2 are samples of independent Gaussian random variables of zero mean and variance $N_0/2$, since (3.20) and (3.21) corresponds to evaluation of the power density spectrum at the values f_i, which equals $N_0/2$.

Accordingly l_2 is the sample value of a Rayleigh distributed random value L_2 /Haykin 83/ which has a distribution as follows:

$$f_{(L_2|1)}(l_2|1) = \frac{2l_2}{N_0}\exp\left(-\frac{l_2^2}{N_0}\right),\ l_2 \geq 0 \tag{3.22}$$

and then l_1 becomes a sample value of a Rician random variable L_1 /Haykin 83/ which has a distribution as follows:

$$f_{L_1|1}(l_1|1) = \frac{2l_1}{N_0}\exp\left(-\frac{l_1^2+E_b}{N_0}\right)I_0\left(\frac{2l_1\sqrt{E_b}}{N_0}\right),\quad l_1 \geq 0 \tag{3.23}$$

where I_0 is the modified Bessel function of the first kind of zero order.

When symbol 1 is transmitted, the receiver makes an error if the sample value of l_2 is exceeds the sample value of l_1. Consequently the probability of this error is obtained by integrating $f_{L2|1}(L_2|1)$ with respect to l_2 from l_1 to infinity and then averaging over all possible values of l_1, i.e:

$$P_{el} = P(l_2>l_1|1) = \int_0^\infty f_{L_1|1}(l_1|1)\left[\int_{l_1}^\infty f_{L_2|1}(l_2|1)dl_2\right]dl_1 \tag{3.24}$$

This is illustrated in Fig. 3.9, where the two probability density functions $f_{L1|1}(l_1|1)$ and $f_{L2|2}(l_2|2)$ are plotted.

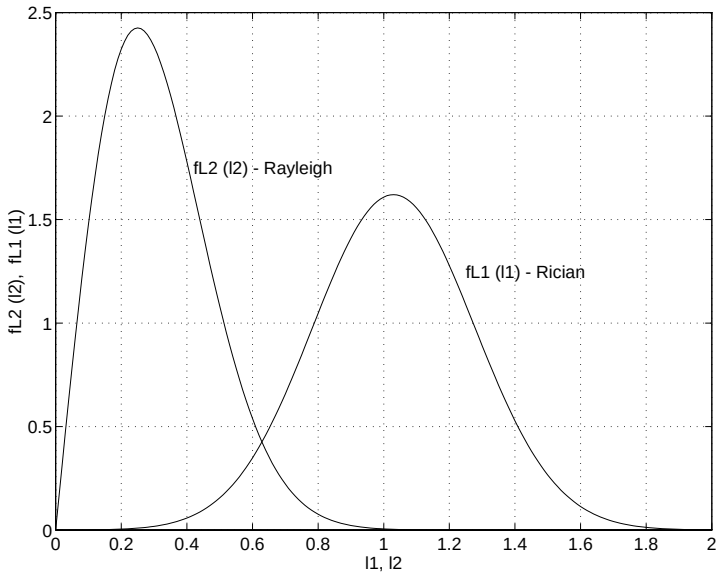

Fig. 3.9 *Probability density functions for the two random variables L_1 and L_2 which are the output of the two channels when symbol 1 was transmitted.*

As can be seen, for a fixed value of l_1, the probability that $l_2>l_1$ can be found by integrating $f_{l2|1}(l_2|1)$ from l_1 to infinity. I.e substituting (3.22) and (3.23) into (3.24) then yields.

$$P_{el} = \int_0^\infty \frac{2l_1}{N_0}\exp\left(-\frac{l_1^2+E_b}{N_0}\right)I_0\left(\frac{2l_1\sqrt{E_b}}{N_0}\right)\left[\int_{l_1}^\infty \frac{2l_2}{N_0}\exp\left(-\frac{l_2^2}{N_0}\right)dl_2\right]dl_1 \tag{3.25}$$

which can be manipulated to equal: /Haykin 83/

$$P_{e1} = \frac{1}{2}\exp\left(-\frac{E_b}{2N_0}\right) \tag{3.26}$$

And similarly when symbol 0 or frequency f_2 is transmitted, the probability that $l_1 > l_2$ (P_{e0}) has by symmetry the same value as (3.26). Thereby the average probability of symbol error for the noncoherent orthogonal FSK equals:

$$P_e = \frac{1}{2}\exp\left(-\frac{E_b}{2N_0}\right) \tag{3.27}$$

This error rate can be plotted along with the coherent counterpart, to show the performance reduction by leaving out information on the phase in the decoding process. This relationship is shown in Fig. 3.10.

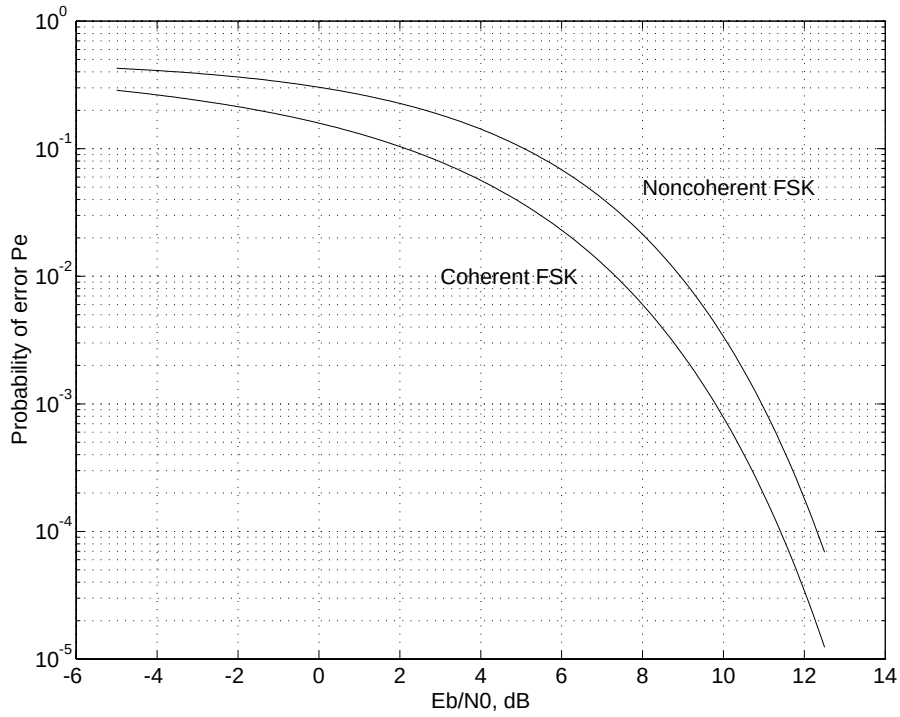

Fig. 3.10 *Theoretical obtainable error rates for Ideal orthogonal Frequency shift keying.*

As can be seen from Fig. 3.10 the coherent orthogonal FSK demodulation signaling technique shows an approximate 1dB better signal to noise ratio immunity for orthogonal signaling. But this is only half the truth. For non-orthogonal FSK modulation which is the case in CCITT V.23, the optimal error rates are different. Theoretical derivation of these error probabilities becomes somewhat tedious when orthogonality no longer is maintained in the transmission. Therefore the case of non-orthogonal FSK is treated by means of simulation in the following.

3.4 Non-Orthogonal Binary Frequency Shift Keying

An analysis of the case where $s_1(t)$ and $s_2(t)$ no longer are orthogonal, can be performed by investigating the actual correlation between the applied frequencies. In Fig. 3.11 a 1300 Hz tone is shown having a duration of $^1/_{1200}$ Sec. - corresponding to one of the symbols in the CCITT V.23 standard.

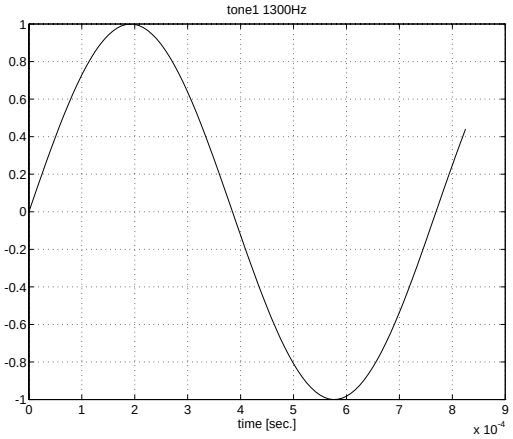

Fig. 3.11 *1300 Hz tone in a bit frame duration of 1/1200 sec.*

The tone in Fig. 3.11 is the correlated with a similar symbol-tone where the resulting correlation coefficient then is plotted versus the second frequency:

$$corr.(f_2) = \frac{\int_0^{T_b} \cos(2\pi 1300t) \cdot \cos(2\pi f_2 t)\, dt}{\int_0^{T_b} \cos^2(2\pi 1300t)\, dt} \qquad (3.28)$$

I.e. the plot shown in Fig. 3.12 is a plot of the correlation coefficient (3.28) as a function of frequency.

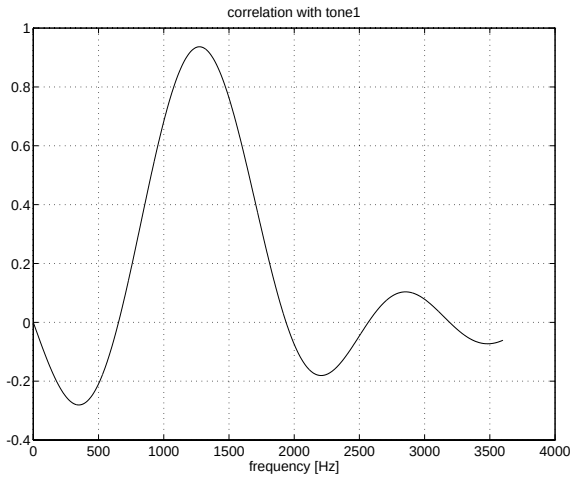

Fig. 3.12 *Correlation between tone 2 with frequency f_2 and tone 1 over 1 bit period. As can be seen for f_2=2100Hz the correlation becomes almost as negative as possible.*

As can be seen from Fig. 3.12 the correlation between the 1300Hz "CCITT - Mark" tone and the other symbol approximately looks as a "sinc" function centered at 1300Hz. It can also be seen that the correlation between the two CCITT tones over one bit-period actually is negative. This means that for coherent signalling the choice of tone-frequencies becomes *better* than if the tones were orthogonal! This is due to the fact that the correlation between orthogonal tones evaluates to zero as a part of the definition. Thereby it can be concluded that the CCITT 1300 and 2100Hz tones will prove better performance than if the tones were chosen orthogonal, e.g. 1200Hz and 2400Hz. But it is also noted that this conclusion only holds for coherent signalling, as the plot shown in Fig. 3.12 corresponds to the phases both equalling zero, i.e. equal. The correlation does not include the sign of the correlation in the noncoherent case, as only the magnitudes of the correlations are compared for discrimination. Thereby it should be evident that the performance of noncoherent signalling using 1300 and 2100Hz as the tone frequencies is lower than for orthogonal symbol tones.

To verify these conclusions a simulation model is constructed using both the coherent and the noncoherent demodulation scheme shown in Fig. 3.7 and Fig. 3.8 respectively. In this simulation the coherent and noncoherent demodulation scheme is combined with both orthogonal and non-orthogonal signalling. The frequencies used are 1200/2400Hz in the orthogonal case and 1300/2100 for the non-orthogonal. To evaluate the performance of the respective signalling forms combined with the demodulation schemes, the error rate is plotted versus the signal to noise ratio. The result of this is shown in Fig. 3.13

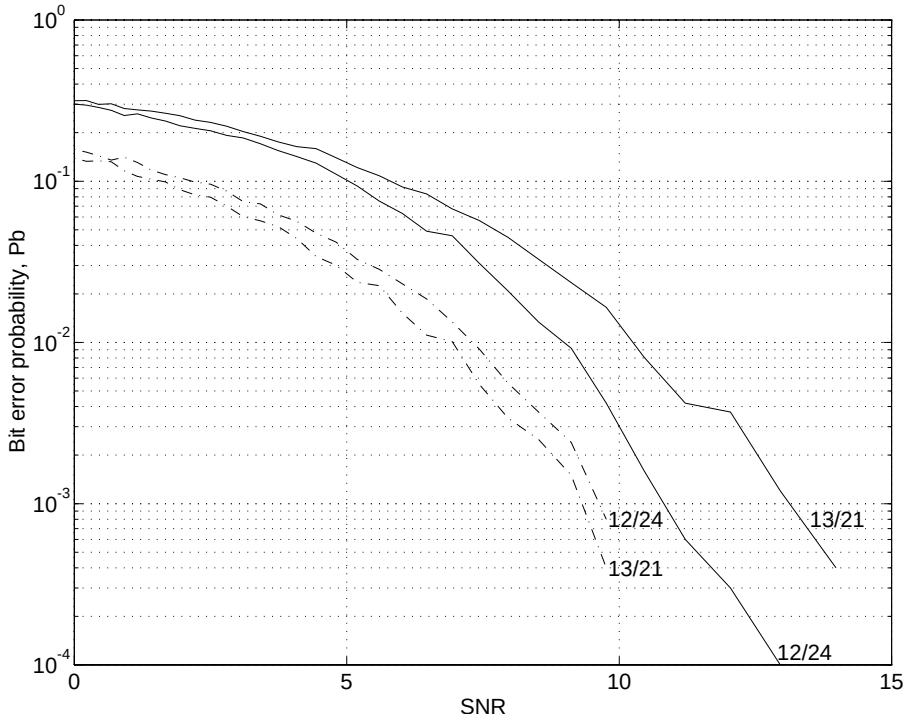

Fig. 3.13 *Error rates for 1200 baud Binary FSK signaling. Solid lines: Non-coherent FSK. Dashed lines: Coherent FSK. 13/21 represents: 1300Hz and 2100Hz, and 12/24 represents: 1200Hz and 2400Hz (SNR=Eb/N_0).*

As can be seen in Fig. 3.13 the orthogonal signalling cases performs as expected in Fig. 3.10. But what is more interesting is the performance of non-orthogonal signalling. As can be seen the coherent demodulation technique performs superior over the others as it includes information about

the phase of the two symbols. This leads as mentioned to even better discrimination than orthogonal signals because of the negative correlation coefficient. The performance of noncoherent demodulation on non-orthogonal is as can be seen lower than for orthogonal signals. This is also in accordance with the conclusion mentioned previously. But to get a closer insight into coherent demodulation technique, the impact of non-perfect phase reconstruction should be considered.

3.5 Non-perfect Phase Reconstruction

To evaluate the impact non-perfect phase reconstruction has on the performance of coherent FSK demodulation, a simulation is constructed similar to the one shown in Fig. 3.13. The difference is that where the coherent demodulation in Fig. 3.13 assumed perfect knowledge of the signal starting phase, the starting phase of the received symbol is varied randomly within certain limits as follows

$$s_i(t) = \begin{cases} \sqrt{\frac{2E_b}{T_b}}\cos(2\pi f_i t + \theta), & 0 \le t \le T_b \\ 0, & elsewhere \end{cases} \tag{3.29}$$

Where theta is a sample value of a uniform distribution limited to the interval -K<θ<K. The following plot shows the error rate obtained when the phase cannot be reconstructed perfectly, i.e the error rate curves are plotted for the values of K=0.1*pi to 0.5*pi in steps of 0.1*pi.

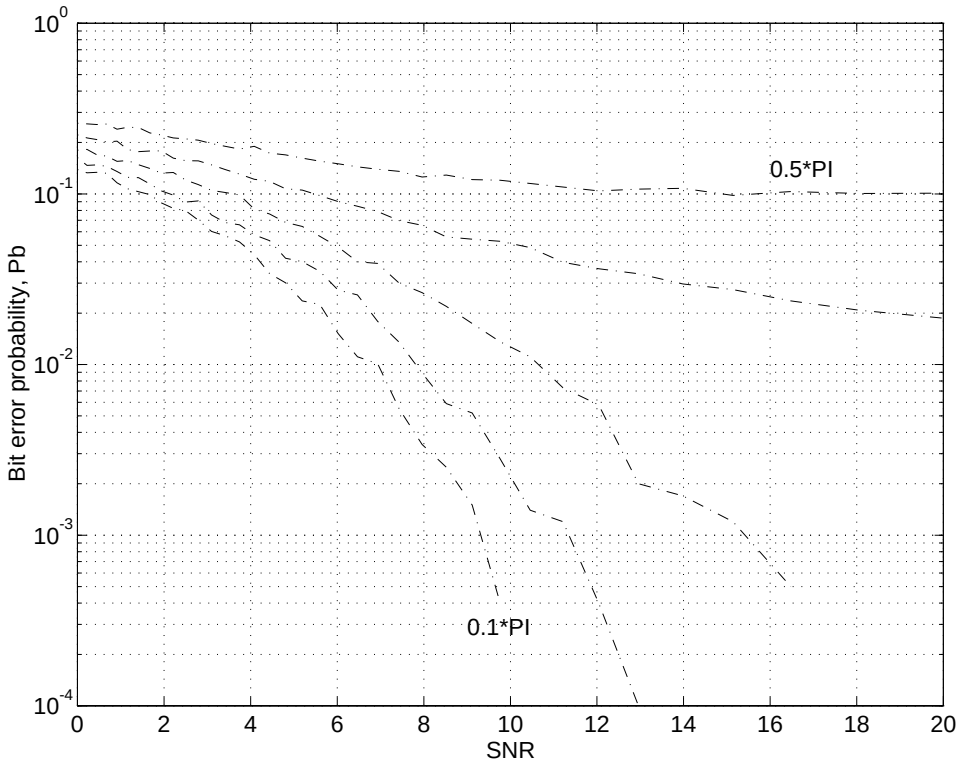

Fig. 3.14 *Error rates for coherent FSK (f_1=1300Hz, f_2=2100) when phase jitter is introduced. The curves plotted show the performance when starting phase is evenly distributed around the correct starting phase. The distribution interval ranges from +/- 0.1*PI (lowermost curve) to +/- 0.5*PI (uppermost curve).*

From Fig. 3.14 it can be seen that small phase derivations from the perfect phase reconstruction only has a minor impact on the bit-error rate of coherent demodulation. But the larger derivations indicate that error-rate increases significantly when the starting phase of the received symbol becomes more and more unknown. The measurements shown in appendix B indicates that for low transmission signal to noise ratios (Fig B.2 in appendix B), the symbol phase may differ as much as simulated in the upper case of Fig. 3.14 and even more. This makes it quite likely that a noncoherent demodulation would outperform the coherent counterpart for these signal levels.

Hereby the discussion of the FSK modulation techniques is ended. The conclusion is that noncoherent demodulation of the non-orthogonal CCITT signalling frequencies will theoretically perform worse than the coherent counterpart. *But* this is only the theoretical part of the case. In practice the performance may very well be different, as the results obtained here on coherent demodulation assumes perfect reconstruction of the signal phase! In most cases this is a very optimistic assumption, and opposed to noncoherent demodulation the coherent demodulation performance is dependent on the quality of the phase reconstruction circuitry. In fact the most difficult part to construct of a coherent demodulator is the phase reconstruction circuit /Johan Broendum[1] - Verbal Source/. And as performance will degrade when deviations from the perfect phase reconstruction occurs, the noncoherent demodulation may be preferred as the theoretical error rate for this signalling technique only depends on the correlation circuit quality. Hence for all digital implementation, the error rate can be determined as a function of wordlength and arithmetic precision!

[1]Johan Broendum is associate professor at Institute of Electronic systems - Department of Telecommunications. His special area of interest is modulation techniques in general and GSM.